

$f_0(980)$ production in $D_s^+ \rightarrow \pi^+ \pi^+ \pi^-$ and $D_s^+ \rightarrow \pi^+ K^+ K^-$ decays

J. M. Dias*

*Departamento de Física Teórica and IFIC, Centro Mixto Universidad de Valencia-CSIC,
Institutos de Investigación de Paterna, Aptdo. 22085, 46071 Valencia, Spain.
Instituto de Física, Universidade de São Paulo, C.P. 66318, 05389-970 São Paulo, SP, Brazil.
E-mail: jorgivan.morais@ific.uv.es*

F. S.Navarra

*Instituto de Física, Universidade de São Paulo, C.P. 66318, 05389-970 São Paulo, SP, Brazil.
E-mail: navarra@if.usp.br*

M. Nielsen

*Instituto de Física, Universidade de São Paulo, C.P. 66318, 05389-970 São Paulo, SP, Brazil.
E-mail: mnielsen@if.usp.br*

E. Oset

*Departamento de Física Teórica and IFIC, Centro Mixto Universidad de Valencia-CSIC,
Institutos de Investigación de Paterna, Aptdo. 22085, 46071 Valencia, Spain.
E-mail: oset@ific.uv.es*

In this work, we have studied the D_s^+ decays into $\pi^+ \pi^+ \pi^-$ and $\pi^+ K^+ K^-$ mesons using the techniques from chiral unitary approach to account for the final state interactions in those processes. For this we have adopted a model in which the D_s^+ meson decays weakly into a π^+ and a quark-antiquark pair $q\bar{q}$, which after hadronization produces two pseudoscalar mesons that undergo final state interactions. As a result, we obtain the invariant mass distributions associated with the pairs $\pi^+ \pi^-$ and $K^+ K^-$, which proceed through $f_0(980)$ decay, and compare them with that ones available from the experiment. Our findings are in a fair agreement with the shape of these experimental data, where a $f_0(980)$ signal is seen in both $\pi^+ \pi^-$ and $K^+ K^-$ distributions. In addition, we have predicted the relative size of these distributions which can be measured by the experimental facilities.

*XVII International Conference on Hadron Spectroscopy and Structure - Hadron2017
25-29 September, 2017
University of Salamanca, Salamanca, Spain*

*Speaker.

1. Introduction

The heavy hadron weak decays which can be produced at B-factories and also at the LHC, have become a valuable source of information on hadron dynamics since we have a big amount of experimental data available which, can be used to test the theoretical models employed to describe the features of hadron dynamics behind those processes. In these decays, many hadron states appears as final states. These latter states can undergo final state interactions (FSI), through which the final particles are formed. The FSI is a complex and important issue in hadron dynamics that can influence all the conclusions concerning new states and it can also play an important role even in CP violation studies [1].

In this work, we study the role of FSI in the invariant mass spectra associated with the D_s^+ decays into $\pi^+ \pi^+ \pi^-$ and also into $\pi^+ K^+ K^-$ mesons [2]. These decays have been studied by several experimental groups [3, 4, 5, 6, 7, 8, 9, 10] and they have been considered excellent tools to study FSI.

2. Theoretical framework

In order to calculate the invariant mass spectra associated with the pair of pseudoscalar mesons $P^+ P^-$ (with $P^+ = \pi^+$ or K^+ and $P^- = \pi^-$ or K^-) mesons are produced via hadronization of a $s\bar{s}$ quark-antiquark pair, as can be seen in Fig. 1, while the other hadron π^+ is considered to be a spectator. Since the original $s\bar{s}$ pair produced in the D_s^+ decay has isospin zero, all the particles which are produced in the hadronization process have also $I = 0$.

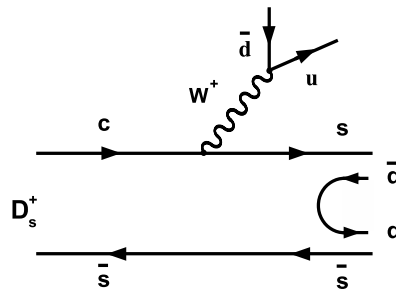


Figure 1: Diagrammatic scheme of the D_s^+ decay at quark level, where we have a π^+ as a spectator and also a quark-antiquark $s\bar{s}$ pair, which is hadronized forming two pseudoscalar mesons. The $q\bar{q}$ pair stands for the isoscalar combination $u\bar{u} + d\bar{d} + s\bar{s}$.

The pair of pseudoscalar mesons formed due to the hadronization of the $s\bar{s}$ pair can be obtained through the matrix M , defined below:

$$M = \begin{pmatrix} u\bar{u} & u\bar{d} & u\bar{s} \\ d\bar{u} & d\bar{d} & d\bar{s} \\ s\bar{u} & s\bar{d} & s\bar{s} \end{pmatrix}, \quad (2.1)$$

which obeys the following relation

$$M \cdot M = M \times (\bar{u}u + \bar{d}d + \bar{s}s). \quad (2.2)$$

In terms of mesons this matrix corresponds to

$$\phi = \begin{pmatrix} \frac{1}{\sqrt{2}}\pi^0 + \frac{1}{\sqrt{3}}\eta + \frac{1}{\sqrt{6}}\eta' & \pi^+ & K^+ \\ \pi^- & -\frac{1}{\sqrt{2}}\pi^0 + \frac{1}{\sqrt{3}}\eta + \frac{1}{\sqrt{6}}\eta' & K^0 \\ K^- & \bar{K}^0 & -\frac{1}{\sqrt{3}}\eta + \sqrt{\frac{2}{3}}\eta' \end{pmatrix}. \quad (2.3)$$

Therefore, in terms of two pseudoscalar mesons produced according to Fig. 1 we find the following correspondence

$$s\bar{s}(\bar{u}u + \bar{d}d + \bar{s}s) \equiv (\phi \cdot \phi)_{33} = K^- K^+ + \bar{K}^0 K^0 + \frac{1}{3}\eta\eta, \quad (2.4)$$

where we have neglected the η' contribution since the mass of η' is too large to be relevant here. These are the states which are produced in the first step, prior to FSI. Once a pair of mesons is created they start to interact and the final $K^+ K^-$ or $\pi^+ \pi^-$ mesons can be formed as a result of complex two-body interactions with coupled channels described by the Bethe-Salpeter equation. In particular, the transition amplitudes $V_{i \rightarrow j}$ between the different pair of mesons are unitarized using them as the kernel of that equation, which in an algebraic form is given by

$$t_{i \rightarrow j}(s) = V_{ij}(s) + \sum_{l=1}^5 V_{il}(s) G_l(s) t_{l \rightarrow j}(s), \quad (2.5)$$

where i and j , which run from 1 to 5, are associated with the channels: 1 for $\pi^+ \pi^-$, 2 for $\pi^0 \pi^0$, 3 for $K^+ K^-$, 4 for $K^0 \bar{K}^0$ and 5 for $\eta\eta$. Furthermore, in Eq. (2.5) G_l is the meson-meson loop function

$$G_l(s) = i \int \frac{d^4 q}{(2\pi)^4} \frac{1}{(p-q)^2 - m_1^2 + i\epsilon} \frac{1}{q^2 - m_2^2 + i\epsilon}, \quad (2.6)$$

with p being the total four-momentum of the $P^+ P^-$ system and, hence, the Mandelstam invariant s is $s = p^2 = M_{inv}^2$. The masses m_1 and m_2 are the masses of the mesons in the loop for the l -channel. The loop function, Eq. (2.6), is regularized by means of a cutoff, which in this work it is equal to 600 MeV.

The differential decay width, as a function of the invariant mass of the pair $P^+ P^-$ is then given by:

$$\frac{d\Gamma_{P^+ P^-}}{dM_{inv}} = \frac{1}{(2\pi)^3} \frac{p_\pi \tilde{p}_P}{4M_{D_s}^2} |T_{P^+ P^-}|^2, \quad (2.7)$$

where

$$p_\pi = \frac{\lambda^{1/2}(M_{D_s}^2, m_\pi^2, M_{inv}^2)}{2M_{D_s}}, \quad (2.8)$$

$$\tilde{p}_P = \frac{\lambda^{1/2}(M_{inv}^2, m_{P^+}^2, m_{P^-}^2)}{2M_{inv}}, \quad (2.9)$$

and

$$\lambda(x^2, y^2, z^2) = x^4 + y^4 + z^4 - 2x^2y^2 - 2x^2z^2 - 2y^2z^2. \quad (2.10)$$

In Eq. (2.9), $m_{p^+} = m_{K^+}$ or m_{π^+} and $m_{p^-} = m_{K^-}$ or m_{π^-} . The amplitudes in Eq. (2.7) are given by

$$T_{K^+K^-} = V_0 \left(1 + G_{K^+K^-} t_{K^+K^- \rightarrow K^+K^-} + G_{K^0\bar{K}^0} t_{K^0\bar{K}^0 \rightarrow K^+K^-} + \frac{2}{3} \frac{1}{2} G_{\eta\eta} \tilde{t}_{\eta\eta \rightarrow K^+K^-} \right), \quad (2.11)$$

with $\tilde{t}_{\eta\eta \rightarrow K^+K^-} = \sqrt{2} t_{\eta\eta \rightarrow K^+K^-}$ and

$$T_{\pi^+\pi^-} = V_0 \left(G_{K^+K^-} t_{K^+K^- \rightarrow \pi^+\pi^-} + G_{K^0\bar{K}^0} t_{K^0\bar{K}^0 \rightarrow \pi^+\pi^-} + \frac{2}{3} \frac{1}{2} G_{\eta\eta} \tilde{t}_{\eta\eta \rightarrow \pi^+\pi^-} \right), \quad (2.12)$$

with $\tilde{t}_{\eta\eta \rightarrow \pi^+\pi^-} = \sqrt{2} t_{\eta\eta \rightarrow \pi^+\pi^-}$.

3. Results

In Fig. 2 we show the amplitude squared $|T_{K^+K^-}|^2$, obtained from Eq. (2.11), as a function of the $K\bar{K}$ invariant mass. We have adjusted the parameter V_0 in order to fit the experimental data, as indicated in Fig. 2 by the dots with error bars. We can see a clear signal related to the $f_0(980)$ resonance, which comes from $|t_{K\bar{K} \rightarrow K\bar{K}}|^2$ on the right-hand side of Eq. (2.11).

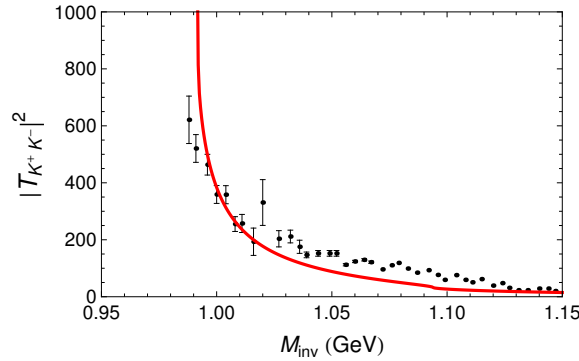


Figure 2: The amplitude squared $|T_{K^+K^-}|^2$ given by Eq. (2.11) as a function of the $K\bar{K}$ invariant mass. The black dots are the experimental results extracted from Ref. [8].

From Fig. 2 we can also see that our theoretical curve reproduce the experimental data around 1 GeV with small discrepancies, which is due to the fact that the experimental data reflects the $f_0(980)$ resonance with mass equals to 922 MeV and 240 MeV for its width, while our results is in good agreement with the ones quoted in the PDG [11].

The numerical results associated with the amplitudes squared $|T_{\pi^+\pi^-}|^2$, as obtained from Eq. (2.12), are shown in Fig. 3 as well as the experimental data for the s-wave contribution for the $\pi^+\pi^-$ invariant mass distribution, extracted from Ref. [9]. The theoretical curve around the $f_0(980)$ peak agrees with the data, but for higher and lower values for the $\pi^+\pi^-$ invariant mass our results are narrower than the experimental ones. One possible reason should be the s-wave contribution associated with the $f_0(1370)$ and $f_0(1500)$ resonances that were not included in our

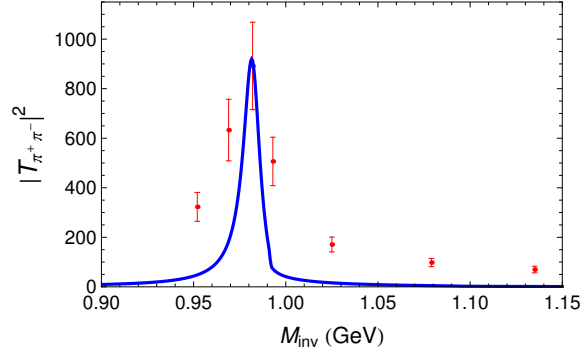


Figure 3: The amplitude squared $|T_{\pi^+\pi^-}|^2$ given by Eq. (2.12) as a function of the $\pi^+\pi^-$ invariant mass. The red dots are the experimental results extracted from Ref. [9].

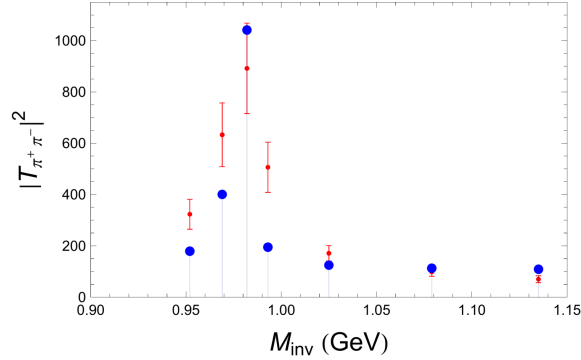


Figure 4: The new amplitude squared $|T_{\pi^+\pi^-}|^2$ as a function of the $\pi^+\pi^-$ invariant mass. The theoretical results, now indicated by the thick dots without error bars, were folded to have the same size of the experimental bins.

calculations. We also do not take into account any source of background in our approach, that comes from the interaction of the pion we are considering as a spectator with the other ones.

Furthermore, the authors in Ref. [9] have considered bins of 15 MeV or more, used to construct the few experimental points in the plot of Fig. 3. In view of this, we consider a theoretical background, which is a constant used to fit the last three experimental points in Fig. 3. In addition, in order to improve the comparison we also integrate our mass distribution over the same bins as experiment, dividing by the size of the bins. As a result, we get a new plot as shown in Fig. 4, where the agreement looks better than the previous comparison, but the experimental data are still broader than the theoretical ones.

In Fig. 5 we make predictions for the relative strength of the rates related with the two reactions, according to Eq. (2.7). As can be seen from Fig. 5, a clear signal associated with the $f_0(980)$ state peaks in the $\pi^+\pi^-$ mass distribution. On the other hand, the K^+K^- distribution gets strength from the underlying $f_0(980)$ close to the $K\bar{K}$ threshold. Experimental measurements related to these two distributions would be useful to compare with our predictions as well as it would be a good test for the chiral unitary approach.

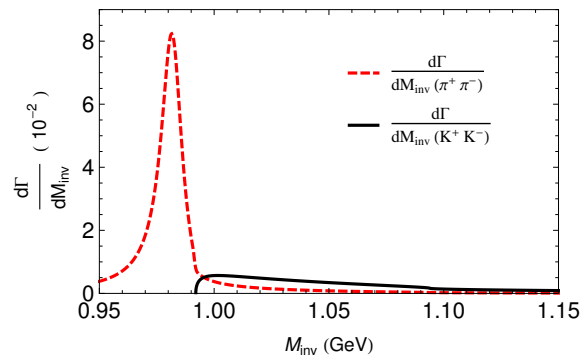


Figure 5: Predictions for the $\pi^+ \pi^-$ and $K^+ K^-$ invariant mass distributions for $D_s^+ \rightarrow \pi^+ \pi^+ \pi^-$, indicated by dashed lines, and also for $D_s^+ \rightarrow \pi^+ K^+ K^-$, solid line curve, with an arbitrary normalization.

4. Conclusions

In this work, we have studied the $D_s^+ \rightarrow \pi^+ \pi^+ \pi^-$ and $D_s^+ \rightarrow \pi^+ K^+ K^-$ decays using the chiral unitary approach to account for final state interactions between the two pseudoscalar mesons, which arise from hadronization of the $q\bar{q}$ component, according to the mechanism we have adopt here and it is illustrated in Fig. 1. As a result, the $f_0(980)$ resonance emerges from the interaction of these two pseudoscalar mesons, which then decays into $\pi^+ \pi^-$ and $K^+ K^-$ mesons. In order to do that we have solved the Bethe-Salpeter equation in coupled channels. We observe that our theoretical curves for $|T_{\pi^+ \pi^-}|^2$ and $|T_{K^+ K^-}|^2$ amplitudes are in a fair agreement with the experimental data reported in Refs. [8, 9], with unavoidable discrepancies for $|T_{K^+ K^-}|^2$ at low values for the $K\bar{K}$ invariant mass due to the small mass of the $f_0(980)$ obtained in Ref. [8]. Furthermore, we also make predictions for the relative strength of the rates of the two reactions that can be measured by the experimental facilities.

References

- [1] J. H. Alvarenga Nogueira, I. Bediaga, A. B. R. Cavalcante, T. Frederico, and O. Loureno, Phys. Rev. **D 92**, 054010 (2015).
- [2] J. M. Dias, F. S. Navarra, M. Nielsen and E. Oset, Phys. Rev. **D 94**, 096002 (2016).
- [3] P. U. E. Onyisi et al. (CLEO Collaboration), Phys. Rev. **D 88**, 032009 (2013).
- [4] A. Zupanc et al. (Belle Collaboration), J. High Energy Phys. 09 (2013) 139.
- [5] J. P. Alexander et al. (CLEO Collaboration), Phys. Rev. **D 79**, 052001 (2009).
- [6] J. P. Alexander et al. (CLEO Collaboration), Phys. Rev. Lett. 100, 161804 (2008).
- [7] P. L. Frabetti et al. (E687 Collaboration), Phys. Lett. **B 407**, 79 (1997).
- [8] P. del Amo Sanchez et al. (BABAR Collaboration), Phys. Rev. **D 83**, 052001 (2011).
- [9] B. Aubert et al. (BABAR Collaboration), Phys. Rev. **D 79**, 032003 (2009).
- [10] E. M. Aitala et al. (E791 Collaboration), Phys. Rev. Lett. 86, 770 (2001).
- [11] C. Patrignani *et al.* [Particle Data Group], Chin. Phys. C **40**, no. 10, 100001 (2016).